coatings

MDPI

Article

Experimental Study on Mechanism, Aging and Fatigue Performance of Warm Mixing Speed Melting SBS Modified Asphalt Binders

Yazhou Zhuang [1], Jinchao Yue [1], Bo Men [2], Guoqi Tang [3] and Riran Wang [1,*]

[1] Yellow River Laboratory, Zhengzhou University, Zhengzhou 450001, China
[2] Henan Xuxin Freeway Co., Ltd., Zhumadian 463000, China
[3] Guolu Gaoke Engineering Technology Institute Co., Ltd., Beijing 100083, China
* Correspondence: wangrr@zzu.edu.cn

Abstract: In this study, two kinds of quick melting modifier SBS-T and SBS-W, as well as the traditional SBS modifier, were used in the optimization design of asphalt binders. The changes in material structure and fatigue properties of three polymer-modified asphalt after adding 3% Sasobit to warm mix agent were investigated. The feasibility of SBS-T and SBS-W in asphalt binder was discussed from the modification mechanism and fatigue properties. In order to reveal the modification mechanism, the interaction mechanism between the fast-melting SBS modifier and the base asphalt was characterized by Fourier transform infrared spectroscopy (FTIR) and X-ray diffraction (XRD). The temperature sensitivity and viscoelastic properties of SBS-T and SBS-W modified binders were determined by frequency scanning (FS). The fatigue properties of SBS-T and SBS-W modified binders were tested by linear amplitude scanning (LAS). The results of FTIR showed that there was no chemical reaction between the SBS-T and SBS-W and the base asphalt. XRD results showed that SBS-W-modified asphalt has stronger fluidity. The results of FS and LAS showed that the asphalt binder with Sasobit has good stiffness and elastic recovery ability, and the same SBS-T and SBS-W have better temperature sensitivity and deformation resistance. In addition, the fatigue life of asphalt binder under the linear viscoelastic continuous damage theory is increased 3.9 times by SBS-W.

Keywords: warm mixed asphalt; speed melting type; viscoelastic characteristic; performance of fatigue; temperature-reduced production and paving of asphalt mixtures

Citation: Zhuang, Y.; Yue, J.; Men, B.; Tang, G.; Wang, R. Experimental Study on Mechanism, Aging and Fatigue Performance of Warm Mixing Speed Melting SBS Modified Asphalt Binders. *Coatings* **2023**, *13*, 311. https://doi.org/10.3390/coatings13020311

Academic Editor: Valeria Vignali

Received: 15 December 2022
Revised: 19 January 2023
Accepted: 20 January 2023
Published: 30 January 2023

1. Introduction

As a kind of advanced pavement with superior performance, asphalt pavement occupies a high proportion in the world of road engineering, it is the general trend to choose the material with excellent performance for asphalt pavement. At present, the scale of freeway construction is increasing day by day, and the modified asphalt can greatly improve the service life of asphalt pavement, and become the necessary material for high-grade road construction [1]. In recent years, the average annual use of asphalt pavement is more than 6 million tons. Since the late 1990s, because SBS (styrene S-butadiene B-styrene S block copolymer) modified asphalt has better performance, gradually become the most used modified asphalt type, accounting for more than 90%. As the common SBS modifier has a high melting point and is not easily dissolved and dispersed, SBS-modified asphalt is generally produced by the wet process invented abroad more than 40 years ago. However, with the deepening of the application, many defects of technology and management are gradually exposed, and environmental protection and safety problems have attracted widespread attention [2]. Wet SBS modification technology not only has high energy consumption, but also has technical defects such as segregation and thermal decomposition, leading to a series of quality management problems [3,4].

If SBS can be used separately from asphalt, SBS can be directly put into the asphalt mixing plant for use, their storage will not deteriorate, their quality and dosage are transparent, and all problems will be solved. This method is the dry direct injection modification technology. Dry method is not a fresh word in fact, it has been throughout the history of the development of modified asphalt, Sweden as early as the 1960s developed asphalt concrete mixed with rubber particles dry production process, rock asphalt, hard petroleum asphalt, and other dry process has been a large number of applications. Because the processing link in the modified asphalt plant is canceled by the dry process, the energy consumption is much less than that produced by the wet process to produce the same amount of modified asphalt [5]. Therefore, the comprehensive promotion of dry modification technology is not only required by the current situation of the industry, but also in response to the call of the state to create technical support for the industry green highway. Guolu Gaoke Engineering Technology Institute Co., Ltd. has developed the first high-performance, low melting point, micron-level rapid melting SBS modified material (SBS-T) in China: the rapid melting SBS modifier is directly put into the asphalt mixing building for use, so that it can be quickly melted in the normal mix, and directly produce SBS modified asphalt mixture.

Generally, the modified asphalt mixture needs to achieve a better modification effect when the stirring temperature is 175–185 °C. This kind of high-temperature mixing not only seriously increases the degree of asphalt aging, but also leads to a serious increase in energy consumption costs, nitrogen and sulfide and other harmful soot emissions increased significantly [6,7]. In order to solve the problem of high construction temperature of modified asphalt mixture, a variety of asphalt warm mixing technologies emerge at the historic moment, which can reduce the construction temperature by 20–30 °C and still can be normally compacted, which is promoted in the industry as an important technical measure of energy saving and emission reduction. Sasobit, manufactured by Sasol-Wax, is an organic warm thermal additive that has been proven to reduce the viscosity of asphalt adhesives [8–11]. Under the background of national carbon neutrality strategy and green highway development of the Ministry of Transport, Guolu Gaoke Engineering Technology Institute Co., Ltd., (Beijing, China) based on the research and development system of dry SBS modifier, combines small molecule SBS with organic viscosity reduction technology. A warm mix dry SBS modifier (SBS-W) was successfully developed, and the integration of SBS modification and the warm mix was realized for the first time in the industry. When in use, SBS-W can be used as an admixture directly into the asphalt mixing building to produce a modified asphalt mixture. Mixing at 160 °C can be fully melted and achieve the modification effect. While reducing the production temperature and spreading temperature of the modified asphalt mixture to nearly 20 °C, the produced asphalt mixture still reaches a similar level to SBS modified asphalt mixture. There is no need to adjust the rolling process. At the same time, the warm mix dry SBS modification technology inherits a series of advantages in the dry SBS technology system, such as "avoiding the performance attenuation problem of modified asphalt, avoiding the ratio phenomenon of modified indicators, reducing the difficulty of quality supervision of modified asphalt mixture", which meets the functional requirements of warm mix and improves the life of asphalt pavement [12].

Asphalt pavement in service will be due to the cyclic action of vehicle load will reduce the strength. When the vehicle load is cycled to a certain number of times, it will make the asphalt pavement crack and cause fatigue failure, so the asphalt fatigue characteristics play a vital role. Daniel has conducted a large number of tests, which show that the viscoelastic damage characteristics of asphalt mixture do not depend on loading conditions, and each material has its specific Damage Characteristic Curve (DCC), which can be determined by simple monotone loading test [13]. Later, scholars such as Underwood have reasonably Simplified the Viscoelastic Continuum Damage (VECD) model (S-VECD) so that it can better analyze the dynamic fatigue test results of asphalt mixture. Thus the asphalt pavement fatigue performance can be evaluated and predicted more accurately [14]. The

whole test process is about 5 min, and the test efficiency is high. It can be used to estimate the fatigue life of asphalt binders at any strain level [15–17].

Hence, this paper has conducted a comprehensive study, in order to select the appropriate modifier to bring excellent performance of asphalt binder to provide guidance. The purpose of this work is to evaluate the modification effects of two fast-melting modifiers (SBS-T and SBS-W) and traditional SBS on asphalt binder, as well as their combined modification effects with Sasobit. To be specific, this work mainly focuses on the following aspects. First, the microscopic characteristics of SBS/SBS-T/SBS-W modifiers and modified binders were characterized by XRD and FTIR infrared spectroscopy to determine the chemical composition and microstructure of the modifiers and further reveal the modification mechanism. Then, the viscoelastic parameters of different kinds of modified asphalt binder were analyzed by FS frequency scanning test, WLF equation and CAM model. Finally, the LAS fatigue acceleration test was carried out by DSR, and the fatigue damage resistance of various modified asphalt in base asphalt binder was studied based on VECD theoretical model.

2. Theoretical Background

2.1. Linear Viscoelastic Theory

Asphalt is a characteristic viscoelastic material. In the range of linear viscoelastic (LVE), its rheological properties are meaningfully impacted by loading conditions, such as temperature and frequency. Whereas, the rheological properties of asphalt binder under disparate loading conditions are often prolonged and labor-intensive. Therefore, the researchers developed a predictive model to measure the rheological arguments of asphalt at random temperatures and frequency, and then used the constitutive equation to calculate the rheological properties.

These models need to apply the time-temperature superposition principle (TTSP). TTSP, known as the time-temperature zoom and frequency-temperature duplication principle, is a very resultful instrument to evaluate the rheological properties of asphalt. TTSP method was used to select the referable temperature T_r, and a continuous curve was obtained by translation fitting. The obtained data were the sweep test data at diverse temperatures in the orientation of the referable temperature. The displacement argument is requested to institute the main curve at det temperature, which is called the temperature displacement factor φ_T. In this paper, the classical WLF nonlinear equation is used to fit the temperature displacement factor φ_T in TTSP.

$$\lg\varphi_T = \frac{-D_1(T - T_r)}{D_2 + (T - T_r)} \tag{1}$$

where T is the test temperature; T_r stands for the referential temperature (25 °C) of the master curves; and the matching arguments of the WLF are denoted as D_1 and D_2.

$$|G^*| = G_g\left[1 + \left(\frac{\omega_c}{\omega_r}\right)^v\right]^{-\frac{m}{v}} \tag{2}$$

where ω_c, m, v are the viscoelastic parameters obtained by the fitting; G_g is the glassy modulus of asphalt materials, taken as 1 GPa in this study; ω_r is the reduced angular frequency, which can be calculated by Equation (3):

$$\omega_r = \varphi_T \times \omega \tag{3}$$

where ω is the test angular frequency.

2.2. S-VECD Model

Many researchers have conducted a lot of experimental studies on the S-VECD theory, and the research consequence shows that the S-VECD theory model can precisely analyze and predict the fatigue damage nature of asphalt materials [18]. Schapery's work potential theory (WPT), which is based on the principle of non reversing thermodynamics, is the theoretical basis for the establishment of the S-VECD model. In this theory the expression of material damage rate is given by Equation (4):

$$\frac{dS}{dt} = \left(-\frac{\partial W^R}{\partial S}\right)^{\alpha} \tag{4}$$

where α is the characteristic constant introduced by Schapery into the theory of the work potential for elastic media materials and later extended to viscoelastic materials. The value of α is also related to the loading mode; Lee and Kim et al. [19] concluded that $\alpha = 1 + 1/m$ in the strain control pattern and $\alpha = 1/m$ in the stress control mode. S is defined as the damage variable to characterize the damage inside the material; t is the test time; the supposititious strain energy density is denoted as W^R, and it can be calculated as Equation (5):

$$W^R = \frac{1}{2} \cdot DMR \cdot C(S) \cdot \left(\gamma_p^R\right)^2 \tag{5}$$

where the dynamic modulus ratio (DMR) is the ratio of the tested initial modulus $|G^*|_{initial}$ to the dynamic state modulus $|G^*|_{LVE}$. This argument was imported to remove the adaptability. The range of DMR is generally from 0.9 to 1.1.

C is the pseudo modulus, then, the relationship between t, C and the damage variable S can be fitted by using Equation (6):

$$C(S) = \frac{\tau_p}{\gamma_p^R \times DMR} \tag{6}$$

where τ_p is the peak shear stress; the peak pseudo strain ${\gamma_p}^R$ during this loading cycle can be calculated by Equation (7):

$$\gamma_p^R = \frac{1}{G_R} \cdot |G^*|_{LVE} \cdot \gamma_p \tag{7}$$

where γ_p is the peak shear strain, and G_R is the reference shear modulus, which is taken as 1 MPa in this study to simplify the calculation process and make the imaginary strain dimensionless.

In combination with Equations (4)–(8), the accumulative variation in the damage variate S over time t is acquired as follows:

$$S(t) = \sum_i^N \left[\frac{DMR}{2}\left(\gamma_p^R\right)^2 (C_{i-1} - C_i)\right]^{\frac{\alpha}{1+\alpha}} [t_{Ri} - t_{Ri-1}]^{\frac{1}{1+\alpha}} \tag{8}$$

$$t_{Ri} = \frac{t_i}{\varphi_T} \tag{9}$$

where i is the loading period, and t_R is the reduced time.

Based on the experimentally measured data, the values of C and S can be calculated, and their relationship between them can be fitted according to Equation (10):

$$C(t) = 1 - C_1 \cdot S(t)^{C_2} \tag{10}$$

where C_1, C_2 are the best-fitting parameter.

2.3. Failure Definition and Criterion for Asphalt Binder

Pseudo strain energy (PSE) theory eliminates the effect of the viscoelasticity of asphalt materials and quantifies the damaging effect caused by the load separately. The test data should be analyzed in pseudo strain coordinates, and Figure 1 shows the definition of the imaginary strain energy in the LAS test. Taking the "undamaged line" as a reference, at the beginning of the test, the mechanical response is the same as that of the "undamaged line", reflecting that the material has not been damaged. With further loading, the strain enlarges step by step and the practical answer of the asphalt tends to deviate from the "undamaged line", demonstrating that the asphalt is getting destroyed and that damage accumulates [20].

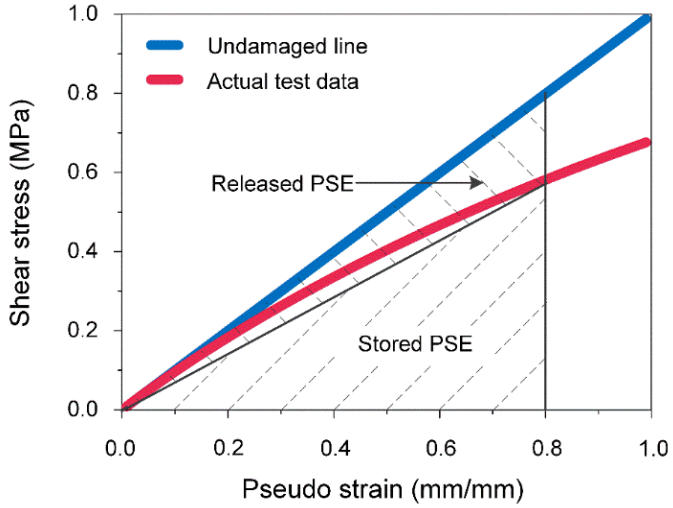

Figure 1. Definition of pseudo strain energy.

Then the stored PSE can be calculated by using Equation (11) for that point, denoted as $W^R{}_s$. The total PSE ($W^R{}_t$) applied to the asphalt from outside during the loading process can be expressed as the area of the triangle enclosed by the trunnion axis, calculated by using Equation (12). Therefore, as an approximation, Equation (13) shows that the PSE released by the material because of $W^R{}_r$ can be calculated by subtracting the hoarded PSE ($W^R{}_s$) from the $W^R{}_t$. $W^R{}_s$ and $W^R{}_r$ can be represented by the two shaded areas in Figure 1.

$$W_s^R = \frac{1}{2} \times \tau_p \times \frac{\gamma_p^R}{DMR} = \frac{1}{2} \times C \times \left(\gamma_p^R\right)^2 \tag{11}$$

$$W_t^R = \frac{1}{2} \times \tau_{undamage} \times \gamma_p^R = \frac{1}{2} \times \left(\gamma_p^R\right)^2 \tag{12}$$

$$W_r^R = W_t^R - W_s^R = \frac{1}{2} \times (1 - C)\left(\gamma_p^R\right)^2 \tag{13}$$

Therefore, with the use of Equations (11)–(13), the values of $W^R{}_s$ and $W^R{}_t$ in the LAS test can be counted for every datum point and the results are plotted in Figure 2. At the beginning of the test, the asphalt can basically store all the PSE input from the load, and $W^R{}_r$ is nearly zero. Throughout the experiment, the amplitude of the loading gradually increases, $W^R{}_s$ increase, and $W^R{}_r$ also increases. The release of energy indicates that the material is gradually being damaged. A sharp peak point in $W^R{}_s$ follows, and after reaching the maximum, it begins to decline, manifesting that the asphalt gradually loses its ability to store energy and release increasing amounts of energy. The maximum value of $W^R{}_s$ is the maximum amount of external energy that the material can store, which characterizes the fatigue performance of the material itself and has a good agreement compared to the phase angle response, so it is considered that fatigue failure occurs in asphalt binder when $W^R{}_s$ reaches a maximum. Then the average $W^R{}_r$ for each cycle, $\overline{W_r^R}$, can be calculated from the

beginning of the test to the fatigue failure of the material. G^R, the PSE release rate during this period, can be calculated by Equation (14):

$$G^R = \frac{\overline{W_r^R}}{N_f} = \frac{\frac{A}{N_f}}{N_f} = \frac{A}{\left(N_f\right)^2} \tag{14}$$

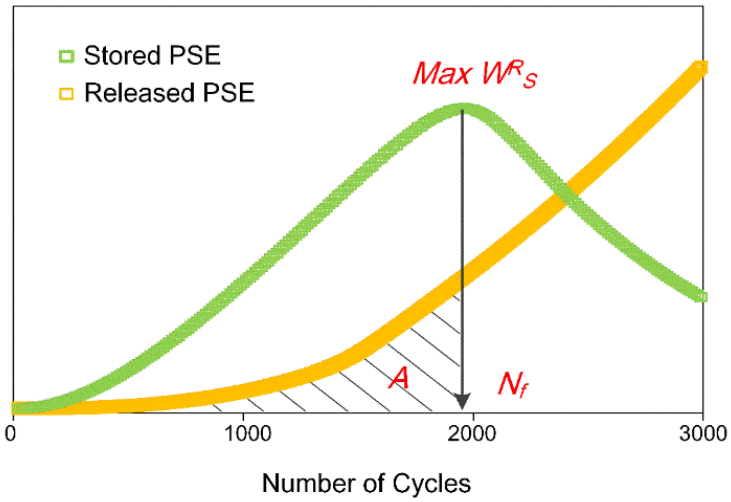

Figure 2. PSE-based failure definition.

As displayed in Figure 2, the shadow area A is the area of the W^R_r curve before fatigue failure. The calculated G^R and its corresponding N_f are plotted on double logarithmic coordinates, and the relationship between G^R and N_f can be well-fitted by a power function [21]:

$$G^R = aN_f{}^b \tag{15}$$

where a and b are the best-fitting parameters.

$$N_f = \left[\frac{K}{a} \times (\gamma)^{2+2\alpha\left(\frac{C_2}{Q}\right)}\right]^{\frac{1}{b+1-\frac{C_2}{Q}}} \tag{16}$$

where K and Q can be counted by Equations (17)–(19).

$$K = \frac{1}{2} \times C_1 \times \left(|G^*|_{LVE}\right)^2 \times P^{\left(-\frac{C_2}{Q}\right)} \times \frac{1}{\left(\frac{C_2}{Q}\right)+1} \tag{17}$$

$$Q = 1 - \alpha \times C_2 + \alpha \tag{18}$$

$$P = \frac{f \times 2^\alpha}{Q(C_1 \times C_2)^\alpha \left(|G^*|_{LVE}\right)^{2\alpha}} \tag{19}$$

P is the calculated parameter. After fitting the test data, the fatigue life of asphalt materials under different strain levels can be predicted.

3. Materials and Test Methods

3.1. Materials

The matrix asphalt with physical properties as shown in Table 1 was selected. Three polymers, SBS, SBS-T and SBS-W, were selected as polymer modifiers, and Sasobit as warm mix agent. The Sasobit modifier, as well as its parameters, was provided by Henan Lupeng Transportation Technology (Zhengzhou, China). The technical information is shown in Table 2. Both SBS, SBS-T, and SBS-W, as well as their parameters, were provided by Beijing Guolu Hi-tech Co., Ltd. (Beijing, China). Table 3 lists the information of all modifiers.

Table 1. Technical information of base asphalt.

Parameters	Units	Values	Technical Requirement
Penetration test	0.1 mm	70	60–80
Softening Point test	°C	51.8	>46
Rotational viscosity (135 °C)	Pa·s	0.63	-
Ductility test	cm	>100	>100

Table 2. Technical information of modifiers.

Modifiers	Parameters	Units	Values
SBS	Oil content	%	0.70
	S/B ratio	-	30/70
	Total ash	%	0.20
	Tensile strength	MPa	18.0
	Voliatility	%	1.00
	Elongation	%	700
Sasobit®	Viscosity at 135 °C	Pa·s	5.47×10^{-3}
	Viscosity at 150 °C	Pa·s	3.26×10^{-3}
	Flashing point	°C	290
	Melting point	°C	100
	Penetration at 25 °C	0.1 mm	1
	Penetration at 60 °C	0.1 mm	8

Table 3. Technical information of fast melting modifiers.

Modifiers	Parameters	Units	Values
SBS-W	Appearance	Particle	-
	Individual weight	g	0.20
	Total ash	%	18.0
	Dry mix dispersibility	-	No particle residue
SBS-T	Appearance	Green particle	-
	Individual weight	g	0.25
	Total ash	%	0.42
	Dry mix dispersibility	-	No particle residue

3.2. Preparation of Sample

Three kinds of polymer-modified asphalt (PMA) were prepared with 5% SBS, 5% SBS-T, and 6% SBS-W as additives. 3% Sasobit, which acted as a warm mixing agent, was added to three polymer-modified asphalt. The primary steps of preparing modified asphalt are as follows: the matrix asphalt is placed in the oven at 120 °C until it is entirely melted, and then SBS or SBS-T or SBS-W modifier is added into the matrix asphalt, and the shear rate is 5000 r/min with a high-speed shear machine for 30 min at 170 °C. Then, after the preliminary of the PMA was completed, a portion of the PMA was heated in an oven for 30 min at 140 °C, in which 3% Sasobit warm mix was added and mixed for 30 min on a high-speed shearing machine at 5000 r/min.

3.3. Microscopic Characteristics

The differences and similarities of the internal crystal phases of SBS, SBS-T, and SBS-W polymer-modified asphalt and the changes of the internal crystal phases of the three polymer-modified asphalt before and after the addition of Sasobit were compared. The sharp X-ray diffractometer (Empyrean) produced by Panaco in Almelo, the Netherlands was used. The target material of the optical tube was Cu-Kα, the tube voltage was 45 KV, and the tube current was 40 mA. The preparation process of the XRD test sample is as follows: the PMA sample is heated to liquid condition, a little amount of asphalt is dropped into the center of the slide, and heat preservation is made to flatten it to form a smooth

surface asphalt film. In this study, the scanning range of diffraction angle (2θ) is 10~90°, the scanning rate is 0.05°/s, and the wavelength is 0.154 nm. A software called MDI Jade 6.5 (V6.5, 2019, Materials Data, Livermore, CA, USA) was used to analyze the test data. XRD tests are conducted in accordance with AASHTO TP101.

Fourier transform infrared spectroscopy (FTIR, Nicolet Continuum, Thermo Fisher Scientific, Waltham, MA, USA) was used to study the variations of their chemical compositions. The preparation process of the infrared spectrum sample is as follows: the modified asphalt sample is dissolved with CS2 organic solution, an amount of the liquor is dropped on the KBr slide, the liquor is completely air seasoning to form asphalt film, and therewith put into the FTIR sample chamber for testing. The frequency of spectral scanning used in this study is 64 times, and the scanning range is 4000–400 cm^{-1}. FTIR tests are conducted in accordance with AASHTO TP101.

3.4. Test Methods

The Discovery HR-1 Dynamic Shear Rheometer (DSR) of the TA instruments (New Castle, DE, USA) was used for all tests. The experiment was focused in the range of medium temperature (10–40 °C). To ensure the precision of the data, every test was repeated three times, and the average value was taken to record the data. Tests were conducted according to AASHTO TP101.

3.5. Aging Methods

In this study, asphalt was first subjected to short-term laboratory aging using a rotating film oven test (RTFOT, ASTM D2872). Then the asphalt residue after the RTFOT test was subjected to PAV and UV aging. The residue of RTFOT was placed on a stainless steel plate according to the asphalt film thickness specified in the test, and then placed in a pressure vessel with 2.1 MPa air pressure, and aged for 20 h at the selected aging temperature of 100 °C. Finally, vacuum degassed the residue. That's how the PAV aging test went.

The specific operation process of the UV aging test is to take a 20 g modified asphalt sample after short-term aging and pour it into a stainless steel asphalt aging dish with a diameter of 140 mm and a depth of 10 mm. In order to ensure the effect of ultraviolet aging, it is automatically leveled and covered with an aging dish in the oven, and the asphalt film with a thickness of about 1 mm can be formed, so that ultraviolet light can be uniformly irradiated on the asphalt film. Then the aging tray containing the modified asphalt sample is placed on the sample rack inside the UV aging chamber. The test temperature was set at 45 ± 0.5 °C, the rotation speed was set at 5 r/min, and the radiation intensity measured by the UV radiation instrument was set at 140 w/m^2. The UV irradiation time is 7 days. The aging methods were carried out according to AASHTO TP101 [22].

3.6. Frequency Scan (FS) Test

FS test can describe the viscoelastic characteristic of asphalt binder at any loading temperature and frequency. A strain control mode and 0.1% strain amplitude were applied at 15 °C, 25 °C, and 35 °C, and the frequency range was selected from 0.1 rad/s to 100 rad/s.

3.7. Linear Amplitude Scanning (LAS) Test

LAS test is based on the VECD accelerated fatigue test theory and has been included in the AASHTO TP101 asphalt anti-fatigue evaluation test specification. In this study, the concept of constant strain amplitude rate (CSR) was adjusted by varying the scanning time in addition to standard LAS tests on raw, PAV aged, and UV-aged asphalt. The scanning times were 500 s and 1000 s, respectively. The test temperature was 25 °C, and the loading frequency was 10 Hz. The CSR of the standard LAS test is equal to 30% of the total strain amplitude in a test time of 300 s divided by 0.01%/s. Then, the CSR values tested in this study are respectively 0.1%/s and 0.06%/s.

Through the above tests, the modification mechanism and fatigue properties of modified asphalt are analyzed, and the following conclusions are drawn.

4. Results and Discussion

4.1. XRD Analysis

Although asphalt itself is not crystal, but is a kind of thick cyclic aromatic hydrocarbon, its feature construction also shows the diffraction pattern of layered crystals like graphite in XRD. There are mainly four diffraction peaks: γ peak, (002) peak, (100) peak and (110) peak. The peaks of the first three peaks are roughly located at 2θ = 20°, 25° and 44°. The γ peak comes from the diffraction phenomenon of saturated hydrocarbon in the asphalt component, and the (002) peak comes from the diffraction phenomenon of aromatic hydrocarbon in the thick ring. The crystallinity of asphalt is positively correlated with the peak value. The XRD patterns of the six compound-modified asphalt are shown in Figure 3.

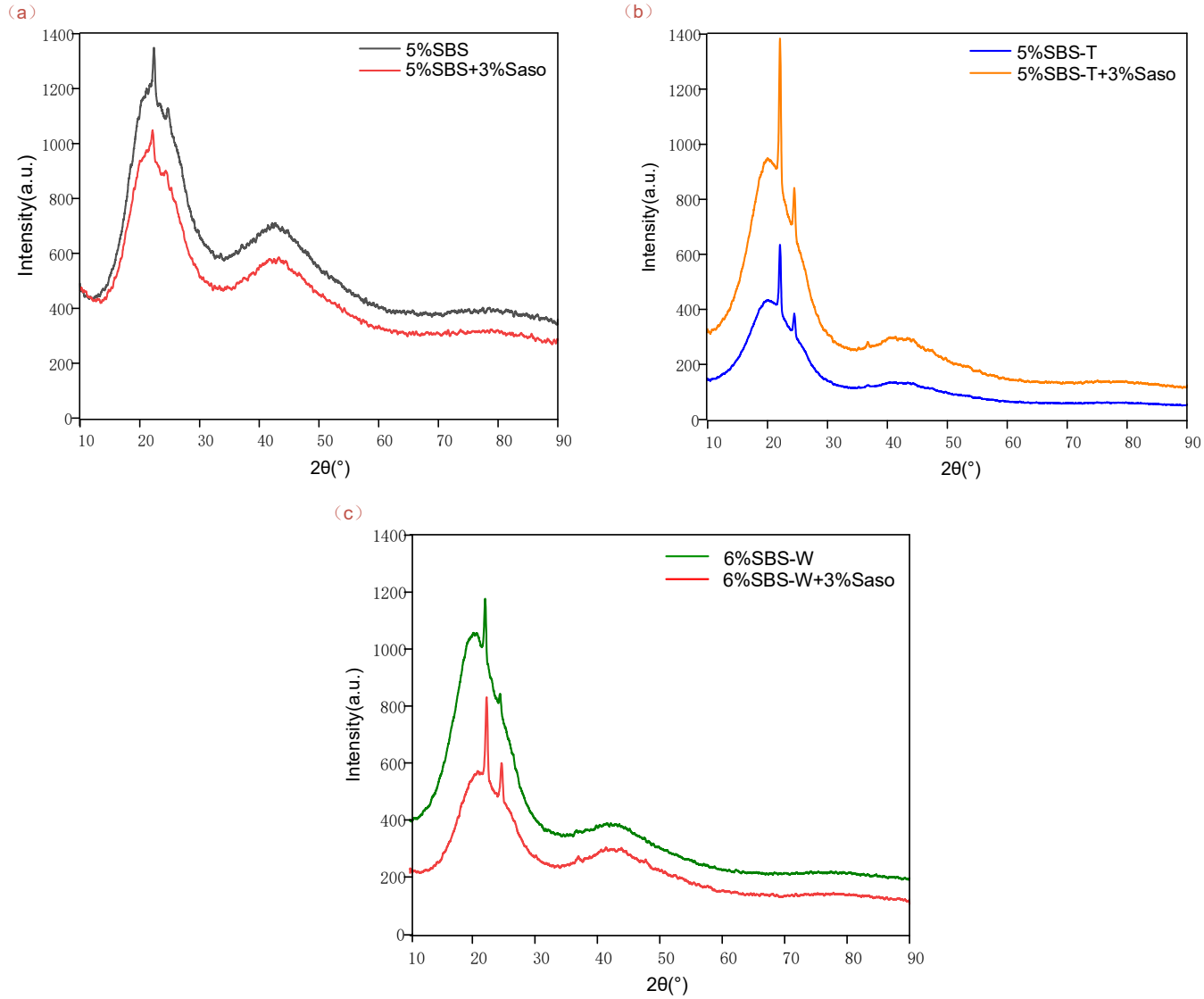

Figure 3. XRD pattern of modified asphalt. (**a**) SBS/Saso; (**b**) SBS-T/Saso; (**c**) SBS-W//Saso.

According to Figure 3a–c, the six modified asphalt all contain substances with the obvious crystal structures. After the addition of Sasobit, no new diffraction peaks appear. All the six modified asphalt samples have γ diffraction peaks near 2θ = 22° and (002) peaks near 2θ = 24°. Before and after SBSMA added 3%Sasobit, the (002) peak was not obvious, indicating that SBS has a strong absorbing ability of aromatic content in asphalt material, and the addition of Sasobit will not have a remarkable effect on it. Nevertheless, after the addition of Sasobit, the γ diffraction peak and (002) peak become more obvious, which indicates that Sasobit will weaken the absorption capacity of saturated and aromatic hydrocarbons in the fast-melting SBS-modified asphalt. MDI Jade 6.5 software was used to analyze the XRD data, and the results of the peak search report were listed in Table 4.

Table 4. XRD peak search report of modified asphalt.

Modified Asphalt Pitch	Distance between Layers (Å)	2θ (°)	Peak Height	Area of Peak	FWHM
5%SBS	3.9685	22.384	255	4194	0.380
	3.5725	24.901	120	2323	0.388
5%SBS+3%Saso	4.0023	22.174	140	4824	0.385
	3.6249	24.537	113	1886	0.186
5%SBS-T	4.0639	21.852	106	1087	0.114
	3.5847	24.817	176	4453	0.282
5%SBS-T+3%Saso	4.0167	22.112	1611	39,164	0.268
	3.6244	24.542	530	12,856	0.232
6%SBS-W	4.0237	22.073	652	10,219	0.281
	3.6436	24.409	215	2969	0.262
6%SBS-W+3%Saso	3.9816	22.310	765	20,496	0.299
	3.6052	24.674	373	11,126	0.333

The XRD pattern shows that the crystal structure of PMA remains intact after the addition of Sasobit. In asphalt binder, the content of saturated fraction and aromatic fraction mainly affect the fluidity of asphalt, and the content of aromatic fraction will make asphalt binder show more viscosity. Therefore, compared with polymer-modified bitumen, the modified asphalt with Sasobit and SBS-W modified asphalt show stronger fluidity on the macro level.

4.2. FTIR Analysis

In order to deeply understand the modification mechanism of the fast-melting SBS modifier on the polymer-modified asphalt binder, this study adopted the Fourier infrared spectrometer model Nicolet Continuum manufactured by Thermo Fisher Science and Technology of the Waltham, MA, USA to analyze the chemical characteristic groups of different types of SBS modified asphalt. In this paper, six kinds of modified asphalt were studied by infrared spectroscopy, and the action mechanism of speed melting SBS modifier polymer modified asphalt was preliminarily determined by analyzing the changes of chemical characteristic groups of asphalt modified by a wet and dry polymer. Figure 4a–c shows the FTIR spectra of SBS-modified asphalt, SBS T modified asphalt, SBS W modified asphalt and the modified asphalt binder with Sasobit added, respectively. The characteristic peak positions of the modified asphalt and the infrared absorption of relevant functional groups are listed in Table 5.

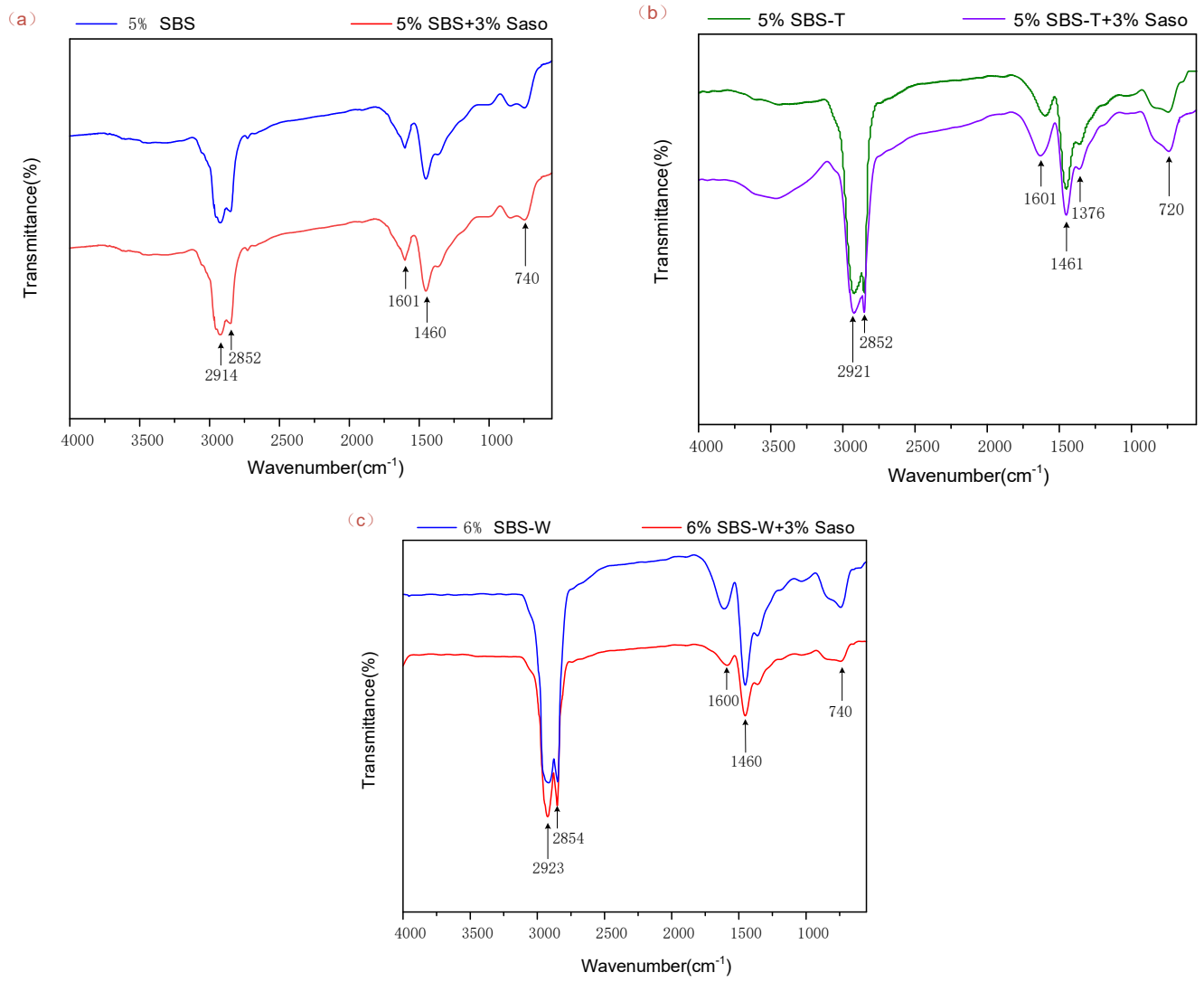

Figure 4. Fourier infrared spectroscopy of modified asphalt. (**a**) SBS/Saso; (**b**) SBS-T/Saso; (**c**) SBS-W//Saso.

Table 5. Characteristic peak information of functional groups of modified asphalt by infrared spectrum.

Characteristic Peak Position	Types of Functional Groups
2921, 2923, 2914 cm^{-1}	Alkanes and cycloalkanes C–H
2854 cm^{-1}	–CH2– Vibration of stretch
1600 cm^{-1}	C=C (Benzene ring skeleton vibration) and C=O
1460–1430 cm^{-1}	–CH3, –CH2–, –CHIn-plane stretching vibration
1376 cm^{-1}	–CH3 Shear vibration absorption peak
800–650 cm^{-1}	Benzene ring substituent C–H

On account of the data information in the chart, the following conclusions can be drawn:

(1) All six asphalt cements have sharp vibration characteristic peaks at about 2925–2850 cm^{-1}, which represents the oscillate assimilate peak of methylene CH2–. It can be observed that the position of characteristic peaks remained unchanged after the addition of Sasobit to the three polymer-modified asphalt, indicating that no complex chemical reaction occurred between Sasobit and the polymer-modified asphalt.

(2) The characteristic peaks of the infrared spectra of SBSMA, SBS-TMA, and SBS-WMA are somewhat different, indicating that SBS and fast-melting SBS additives have different reactions with the base asphalt. SBS-TMA has a weak peak at 1376 cm^{-1}, which is caused by the shear vibration of the methyl group in the SBS-T copolymer molecular chain. Because the proportion of SBS-T copolymer in asphalt is relatively small, so the characteristic peak here is not obvious.

(3) The three polymer-modified asphalts have obvious characteristic peaks at 738 cm^{-1}, and the characteristic peaks at 738 cm^{-1} are the benzene ring =CH. Due to the small proportion of the characteristic peak in the modified asphalt, the characteristic peak is weak.

(4) After the addition of 3%Sasobit, the absorption peaks of the three polymer-modified asphalt were increased in the range of 2930–2800 cm^{-1}, because the content of saturated hydrocarbons was relatively high. This phenomenon may occur due to Sasobit's reduced capacity of the polymer additive to absorb saturated HC in the base asphalt.

4.3. G and δ Master Curves*

Table 6 shows the logarithmic value of the shift factor when 25 °C is the reference temperature. The constructed *G** main curve is shown in Figure 5. As can be seen from Figure 5 as a whole, for the three SBS composite modified binders, the higher the content, the higher the dynamic modulus response. At the same loading frequency, the addition of Sasobit significantly improves the dynamic modulus, especially in the low/high-temperature range. This indicates that the addition of Sasobit can improve the stiffness and high-temperature deformation resistance of polymer-modified asphalt. Under the original condition, the dynamic modulus of the bituminous binder with the mixture ratio of SBS-WMA is the highest when Sasobit is not added, which indicates that the high temperature rutting resistance and low-temperature resistance of the composite modified bituminous binder are the best. The dynamic modulus of SBSMA at high frequency/low temperature is higher than that of SBS-TMA, indicating that SBSMA has brilliant properties at low temperatures. The dynamic modulus of SBS-TMA at low frequency/high temperature is higher than that of SBSMA, indicating that SBS-TMA has better anti-rut performance at high temperature [23]. By comparing the data in Figure 5a,c, it can be found that *G** of PAV aging binder is higher than that of UV aging binder. The fitting parameters m, D1, D2, and so on were obtained from the G^* main curve of the modified binder, and the specific values were shown in Table 7.

Table 6. Fitting parameters of WLF equation.

Asphalt Condition	WLF Fitting Parameters	5%SBS	5%SBS+3%Saso	5%SBS-T	5%SBS-T+3%Saso	6%SBS-W	6%SBS-W+3%Saso
Origin	D_1	28.132	32.455	36.78	37.496	27.188	33.727
	D_2	231.466	251.461	289.73	346.297	264.120	301.786
PAV	D_1	28.893	37.471	33.707	35.114	28.018	34.452
	D_2	258.890	290.873	298.747	289.434	250.125	281.156
UV	D_1	28.073	29.698	27.756	33.718	23.267	29.405
	D_2	230.688	330.426	252.773	298.458	213.281	237.465

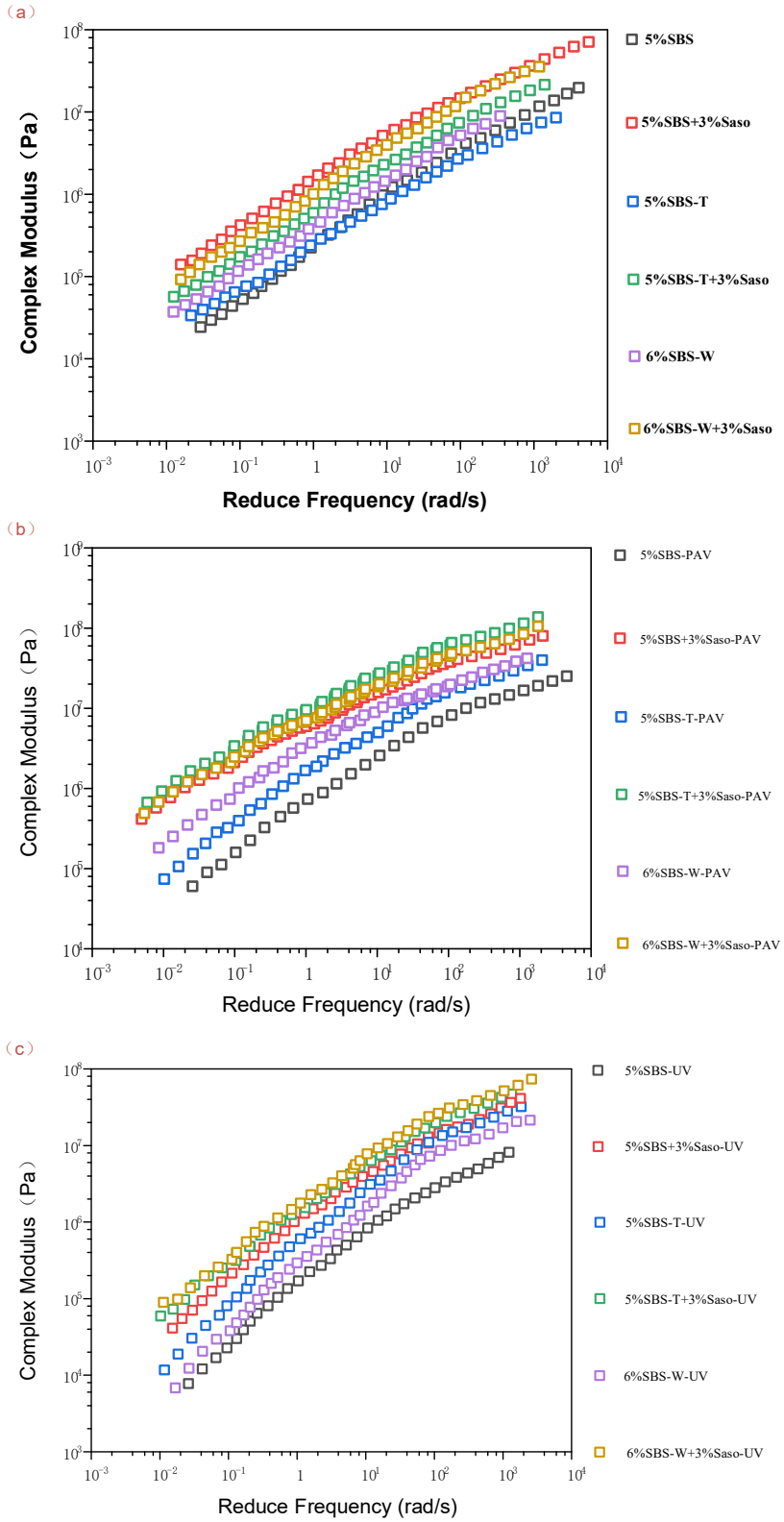

Figure 5. Main curve of dynamic modulus of modified asphalt. (**a**) SBS/Saso; (**b**) SBS-T/Saso; (**c**) SBS-W//Saso.

Table 7. CAM equation fitting parameters of modified asphalt.

Asphalt Condition	CAM Fitting Parameters	5%SBS	5%SBS+3%Saso	5%SBS-T	5%SBS-T+3%Saso	6%SBS-W	6%SBS-W+3%Saso
Origin	ω_c	0.306	0.425	0.673	0.266	0.010	0.006
	m	1.721	1.697	1.469	1.371	1.289	1.157
	v	0.147	0.144	0.149	0.147	0.153	0.161
PAV	ω_c	0.790	0.740	0.415	0.448	0.480	0.340
	m	1.161	1.135	1.138	1.112	1.270	1.167
	v	0.120	0.118	0.134	0.131	0.142	0.144
UV	ω_c	0.312	0.747	0.729	0.689	1.100	0.138
	m	1.710	1.552	1.549	1.445	1.283	1.226
	v	0.142	0.142	0.143	0.143	0.154	0.156

4.4. Stress-Strain Curve

Figure 6 describes the stress-strain response of three composites modified asphalt binders under LAS fatigue tests at two aging levels. The shear stress of all the modified binders showed obvious peaks of different width amplitudes. It has been shown that the wider the peak stress width is, the greater the deformation the asphalt binder can bear. Usually, this change in width is most likely due to a change in the asphalt composition to resist deformation [24,25].

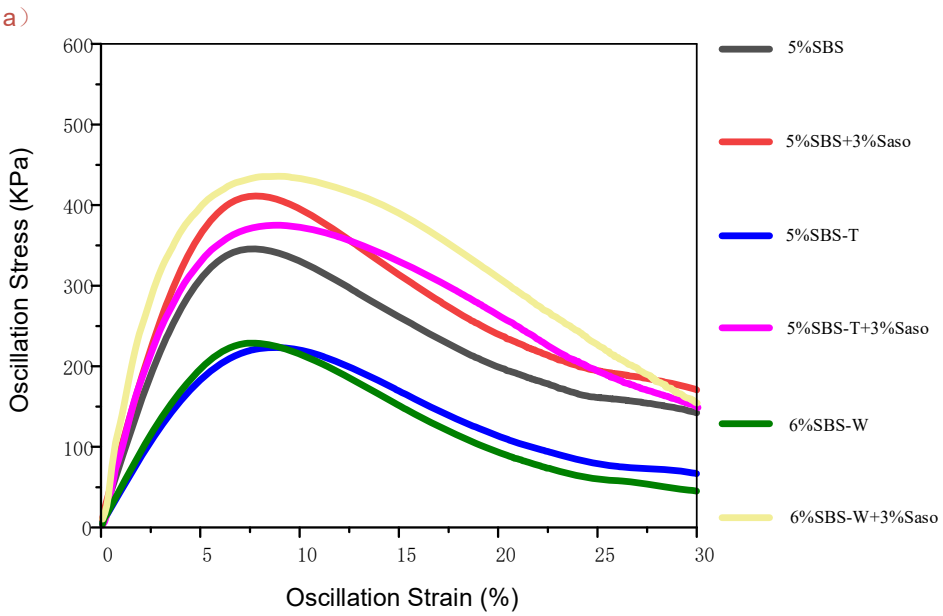

Figure 6. *Cont.*

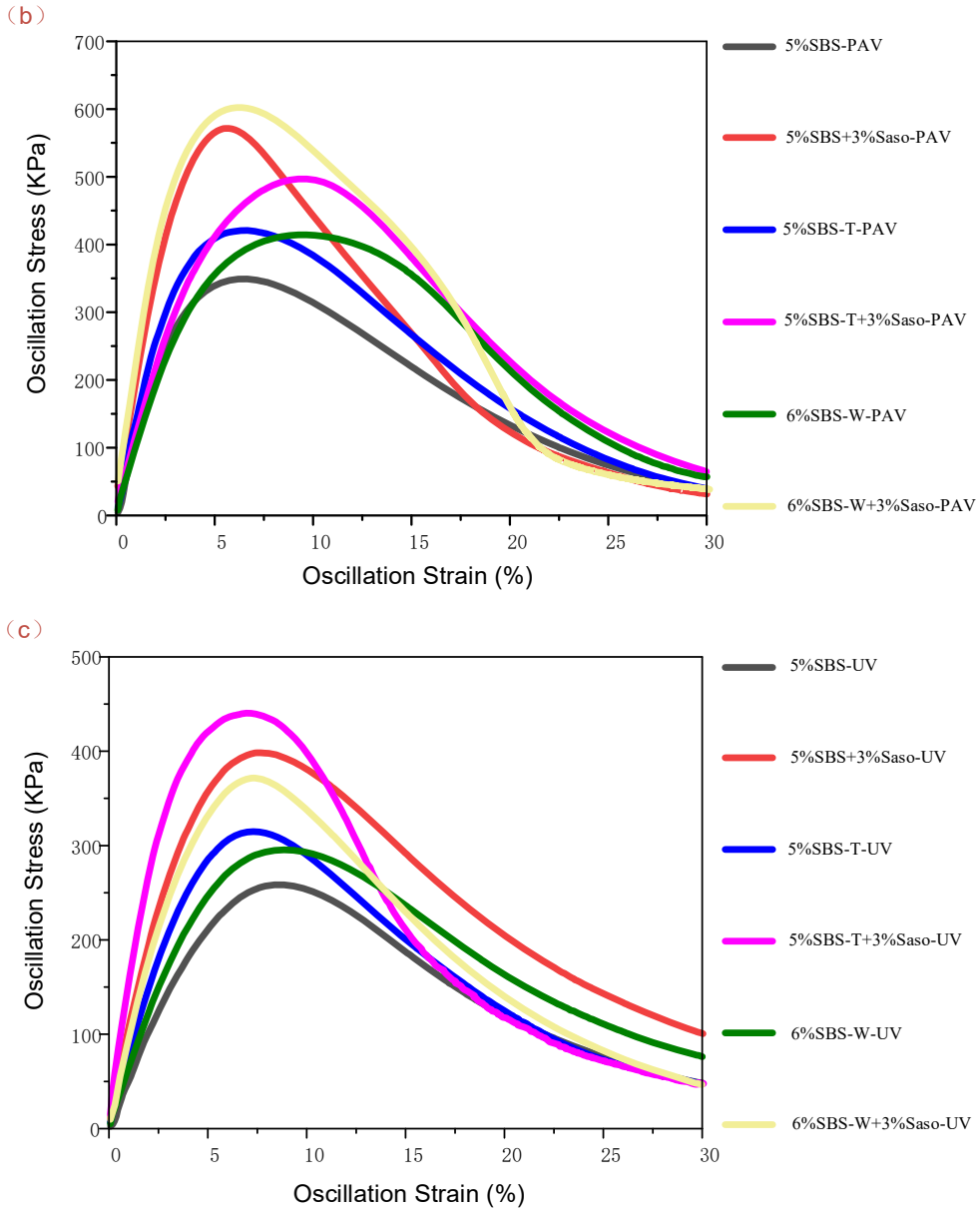

Figure 6. Stress-strain curves of modified asphalt. (**a**) SBS/Saso; (**b**) SBS-T/Saso; (**c**) SBS-W//Saso.

The curves in the figure show that the peak stress and peak width of polymer-modified asphalt after adding Sasobit are significantly increased, which indicates that Sasobit can improve the stiffness and deformation resistance of asphalt binder. Figure 6b,c both show that the strength of UV- or PAV-SBS MA is lower than that of SBS-T or SBS-W modifiers. These results indicate that compared with SBSMA, the speed-melting SBS-modified asphalt has better strength after aging, that is, better fatigue resistance.

4.5. Damage Characteristic Curve

On the basis of PSE theory, the variation trend of the virtual modulus C and damage variable S of the modified asphalt material in the process of fatigue test can be calculated according to the formula, that is, the damage characteristic curve (DCC) of the material.

It can be clearly seen from Figure 7 that with the progress of the experiment, the asphalt binder gradually develops from the undamaged state of C = 1 to the damaged state, and the value of C gradually decreases while the value of S gradually increases. This change can quantify the damage evolution process of the material. The shape of the DCC curve of asphalt binder before and after adding Sasobit is different, indicating that Sasobit

changes the injure evolution process of asphalt. As can be seen from Figure 7a, the DCC curves of the three types of modified asphalt with Sasobit are all above the three types of polymer modified asphalt, indicating that at the same damage degree, the integrity of the warm mixed polymer modified asphalt is better and the ability to resist deformation is stronger. When fatigue failure is reached, the values of the virtual modulus C_f and damage variable S_f of each material are different. Compared with the three polymer-modified asphalt cement, the Sasobit-added asphalt binder has a smaller C_f value and a larger S_f value. Since the virtual modulus C represents the integrity of the material and the damage variable S represents the damage degree of the material, this situation indicates that the material with Sasobit has a larger damage degree when it reaches fatigue failure, and the material has a strong anti-fatigue ability.

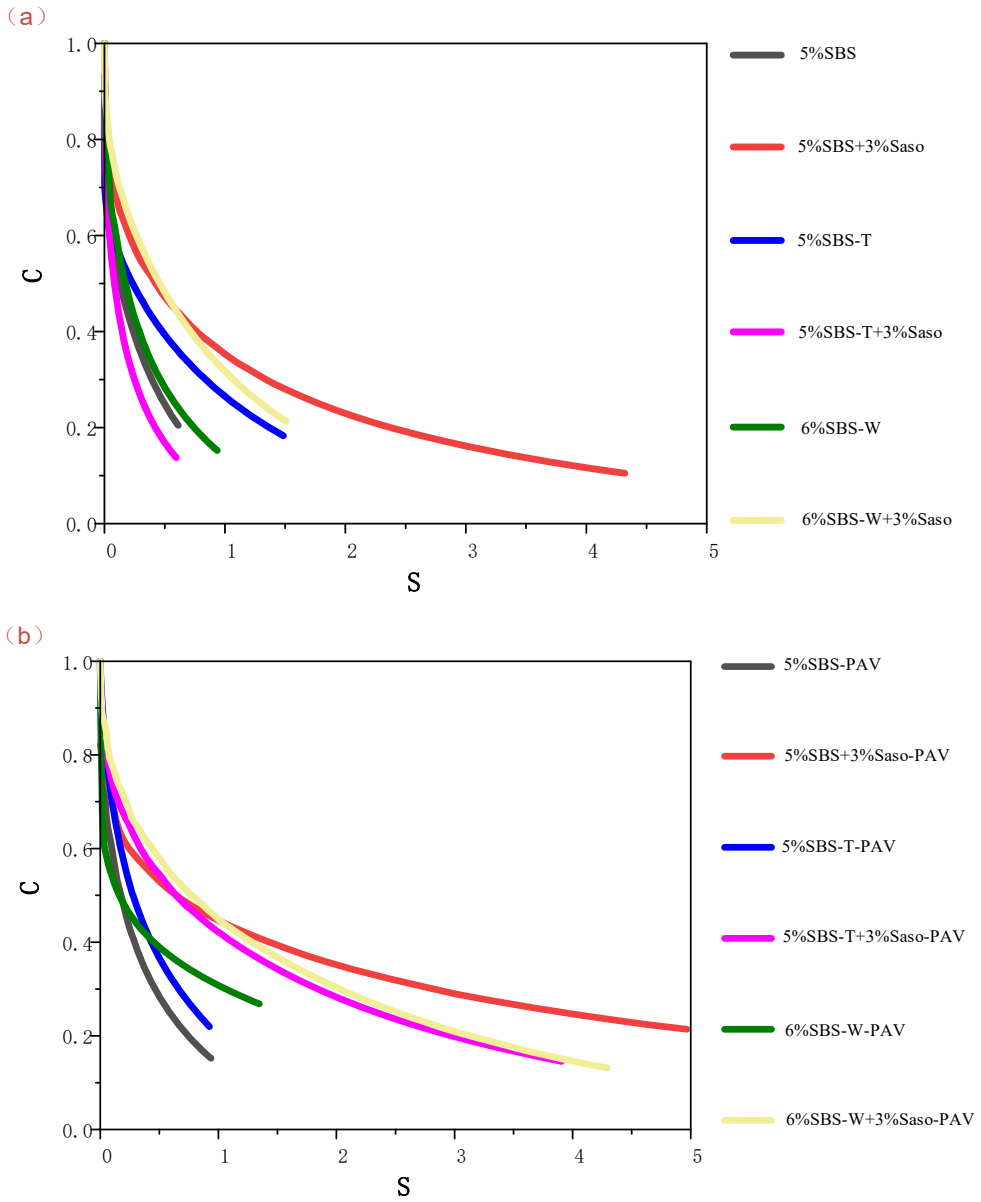

Figure 7. *Cont.*

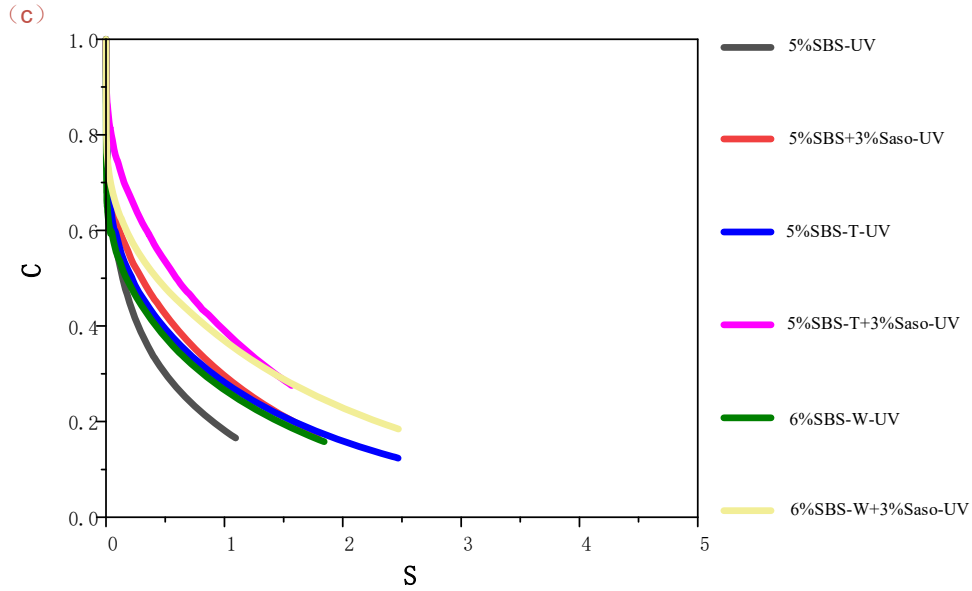

Figure 7. DCC curves of modified asphalt binder: (**a**) SBS/Saso; (**b**) SBS-T/Saso; (**c**) SBS-W//Saso.

The results show that the speed-melting SBS modified asphalt has better fatigue properties than SBS MA at the same strain level, especially under the condition of uv aging. This indicates that compared with the traditional SBS modifiers, the oxidation degree of SBS T and SBS W modifiers is lower in the UV aging process.

As can be seen from Table 8, when the damage variable S is the same, the lower the values of C1 and C2 are, the higher the comparative virtual modulus C is. According to the data, C1 and C2 values decreased after Sasobit was added into the three polymer modified asphalt, indicating that Sasobit can improve the fatigue resistance of polymer modified asphalt, which is consistent with the results shown in the DCC curve image.

Table 8. DCC curve fitting parameters.

Asphalt Condition	Fitting Parameters	5%SBS	5%SBS+3%Saso	5%SBS-T	5%SBS-T+3%Saso	6%SBS-W	6%SBS-W+3%Saso
Origin	C_1	0.628	0.625	0.737	0.731	0.878	0.724
	C_2	0.267	0.237	0.221	0.216	0.236	0.230
PAV	C_1	0.768	0.598	0.842	0.821	0.572	0.555
	C_2	0.350	0.160	0.286	0.267	0.260	0.255
UV	C_1	0.699	0.679	0.603	0.598	0.737	0.642
	C_2	0.232	0.215	0.330	0.208	0.194	0.183

4.6. Fatigue Performance Analysis of Asphalt

According to the values of a and b in Table 9, the fatigue lives of different types of modified asphalt cements at 3%, 6%, and 9% strain levels were calculated and plotted in Figure 8a–c.

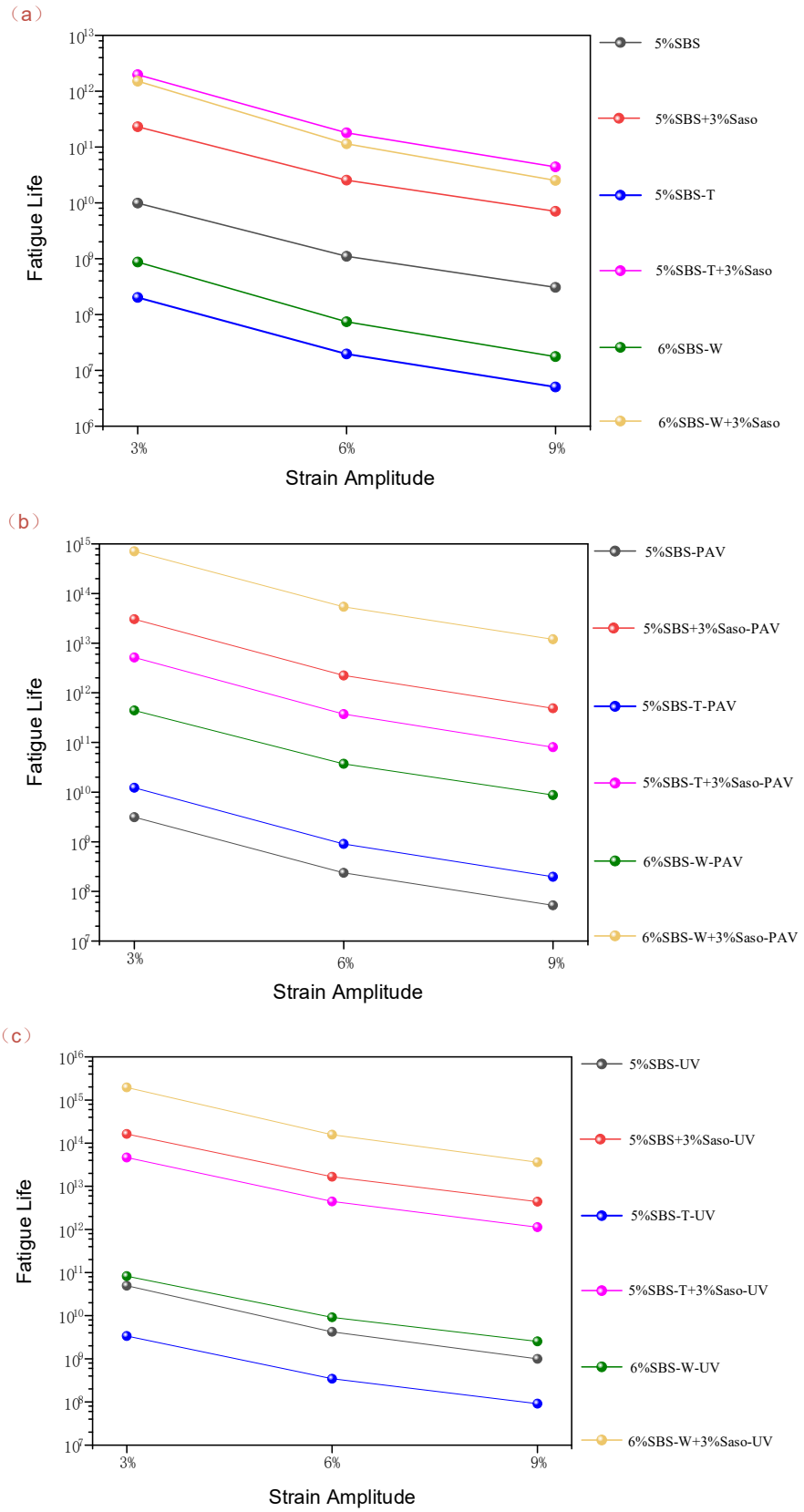

Figure 8. Fatigue life of modified asphalt binder under different strain levels. (**a**) SBS/Saso; (**b**) SBS-T/Saso; (**c**) SBS-W//Saso.

Table 9. Fatigue equation parameters of the binders.

Asphalt Condition	Fitting Parameters	5%SBS	5%SBS+3%Saso	5%SBS-T	5%SBS-T+3%Saso	6%SBS-W	6%SBS-W+3%Saso
Origin	a	2.99×10^{8}	3.03×10^{7}	3.54×10^{10}	1.87×10^{7}	3.63×10^{9}	5.92×10^{9}
	b	−1.841	−2.087	−1.646	−3.644	−2.048	−3.096
PAV	a	9.97×10^{11}	6.32×10^{10}	4.62×10^{10}	3.09×10^{10}	3.48×10^{10}	2.42×10^{7}
	b	−5.114	−4.077	−1.553	−1.963	−2.046	−3.383
UV	a	2.36×10^{10}	2.71×10^{10}	3.45×10^{10}	1.94×10^{9}	3.13×10^{10}	1.66×10^{9}
	b	−1.745	−1.537	−2.059	−1.547	−1.497	−1.547

As can be seen from Figure 8, the fatigue life of the modified asphalt binder after Sasobit is added significantly increases, indicating that Sasobit improves the fatigue resistance of the polymer-modified asphalt. As shown in Figure 8a, the fatigue life of SS-T modified asphalt and SS-W modified asphalt with Sasobit is larger than that of SBSMA under non-aging conditions, indicating that the anti-fatigue performance is better than that of SBSMA. Under the conditions of PAV aging and UV aging, the fatigue life of SBS-W-modified asphalt is the maximum. It can be seen that the speed melting SBS modified asphalt has better fatigue damage resistance.

5. Conclusions

The purpose of this work is to evaluate the modification effects of two fast-melting modifiers (SBS-T and SBS-W) and traditional SBS on asphalt binder, as well as their combined modification effects with Sasobit. First, the microscopic characteristics of SBS/SBS-T/SBS-W modifiers and modified binders were characterized by XRD and FTIR infrared spectroscopy to determine the chemical composition, microstructure, and defect level of the modifiers and further reveal the modification mechanism. Then, the viscoelastic parameters of different kinds of modified asphalt binder were analyzed by FS frequency scanning test, WLF equation and CAM model. Finally, the LAS fatigue acceleration test was carried out by DSR, and the fatigue damage resistance of various modified asphalt in base asphalt binder was studied based on VECD theoretical model. The main findings are as follows:

(1) According to the XRD diffraction peak data, the peak height of the fast-melting modified binders (SBS-T and SBS-W) is higher, their crystallization properties are better, and their crystal phase content is higher than that of the control SBS MA. With the addition of Sasobit, the crystal structure in PMA remains intact. FTIR showed that no chemical changes occurred after Sasobit was added to the asphalt binder.

(2) Compared with SBSMA, the speed-melting modifiers (SBS-T and SBS-W) have higher complex modulus, better fatigue resistance, and lower temperature sensitivity. SBS-W improves stiffness and stability by three times. The addition of Sasobit can also improve the stiffness and stability of polymer-modified asphalt.

(3) The LAS test based on the linear VECD theoretical model shows that the modified asphalt with 6%SBS-W+3%Sasobit mixture ratio has the longest fatigue life, indicating that it has the best anti-fatigue failure ability. The fatigue life is increased 3.9 times by SBS-W. In addition, Sasobit can prolong the fatigue life of asphalt binders.

6. Recommendations

In future research, we will increase the scale to study the fatigue properties of the fast-melting modified asphalt mixture. Sasobit is relatively expensive, and future projects will use more SBS-W, an inexpensive warm mix modifier.

Author Contributions: Y.Z.: Methodology, Investigation, Writing—original draft. J.Y.: Data curation. B.M.: Data curation. G.T.: Resources. R.W.: Validation. All authors have read and agreed to the published version of the manuscript.

Funding: Funding support from the Project of the Henan Provincial Department of Transportation (Grant No. 2021-2-13) and the Key Science and Technology Project of Henan Province (Grant No. 212102310937) were greatly appreciated.

Institutional Review Board Statement: Not applicable.

Informed Consent Statement: Not applicable.

Data Availability Statement: Not applicable.

Conflicts of Interest: The authors declare no conflict of interest.

References

1. Sukhija, M.; Saboo, N. A comprehensive review of warm mix asphalt mixtures-laboratory to field. *Constr. Build. Mater.* **2021**, *274*, 121781. [CrossRef]
2. Zhu, J.; Birgisson, B.; Kringos, N. Polymer modification of asphalt: Advances and challenges. *Eur. Poly. J.* **2014**, *54*, 18–38. [CrossRef]
3. Yu, H.; Chen, Y.; Wu, Q.; Zhang, L.; Zhang, Z.; Zhang, J.; Miljković, M.; Oeser, M. Decision support for selecting optimal method of recycling waste tire rubber into wax-based warm mix asphalt based on fuzzy comprehensive evaluation. *J. Clean. Prod.* **2020**, *265*, 121781. [CrossRef]
4. Cao, R.; Leng, Z.; Yu, H.; Hsu, S.C. Comparative life cycle assessment of warm mix technologies in asphalt rubber pavements with uncertainty analysis. *Resour. Conserv. Recycl.* **2019**, *147*, 137–144. [CrossRef]
5. Mao, Y.; Liu, Y.; Hao, P.W.; Wang, H.N. Process Parameters of Rubber Powder Particles Modified Asphalt. *Adv. Mater. Res.* **2014**, *900*, 491–498. [CrossRef]
6. Ali, B. A review of the warm mix asphalt (WMA) technologies: Effects on thermo-mechanical and rheological properties. *J. Clean. Prod.* **2020**, *259*, 120817.
7. Abd, D.M.; Al-Khalid, H.; Akhtar, R. An investigation into the impact of warm mix asphalt additives on asphalt mixture phases through a nano-mechanical approach. *Constr. Build. Mater.* **2018**, *189*, 296–306. [CrossRef]
8. Xiao, F.; Punith, V.S.; Amirkhanian, S.N. Effects of non-foaming WMA additives on asphalt binders at high performance temperatures. *Fuel* **2012**, *94*, 144–155. [CrossRef]
9. Ameri, M.; Afshin, A.; Shiraz, M.E.; Yazdipanah, F. Effect of wax-based warm mix additives on fatigue and rutting performance of crumb rubber modified asphalt. *Constr. Build. Mater.* **2010**, *262*, 120882. [CrossRef]
10. Yu, H.; Zhu, Z.; Leng, Z.; Wu, C.; Zhang, Z.; Wang, D.; Oeser, M. Effect of mixing sequence on asphalt mixtures containing waste tire rubber and warm mix surfactants. *J. Clean. Prod.* **2020**, *246*, 119008. [CrossRef]
11. Yang, X.; You, Z.; Hasan, M.R.M.; Diab, A.; Shao, H.; Chen, S.; Ge, D. Environmental and mechanical performance of crumb rubber modified warm mix asphalt using evotherm. *J. Clean. Prod.* **2017**, *159*, 346–358. [CrossRef]
12. Yue, M.; Yue, J.; Wang, R.; Xiong, Y. Evaluating the fatigue characteristics and healing potential of asphalt binder modified with Sasobit and polymers using linear amplitude sweep test. *Constr. Build. Mater.* **2021**, *289*, 123054. [CrossRef]
13. Wang, R.; Xiong, Y.; Yue, M.; Hao, M.; Yue, J. Investigating the effectiveness of carbon nanomaterials on asphalt binders from hot storage stability, thermodynamics, and mechanism perspectives. *J. Clean Prod.* **2020**, *276*, 124180. [CrossRef]
14. Bahia, H.U.; Zhai, H.; Bonnetti, K.; Kose, S. Non-linear viscoelastic and fatigue properties of asphalt binders. *J. Assoc. Asph. Paving Technol.* **1999**, *68*, 1–34.
15. Bahia, H.U.; Zhai, H.; Zeng, M.; Hu, Y.; Turner, P. Development of binder specification parameters based on characterization of damage behavior. *J. Assoc. Asph. Paving Technol.* **2002**, *70*, 442–470.
16. Zhou, F.; Mogawer, W.; Li, H.; Andriescu, A.; Copeland, A. Evaluation of fatigue tests for characterizing asphalt binders. *J. Mater. Civ. Eng.* **2013**, *25*, 610–617. [CrossRef]
17. Wang, C.; Castorena, C.; Zhang, J.; Richard Kim, Y. Unified failure criterion for asphalt binder under cyclic fatigue loading. *Road Mater. Pave. Des.* **2015**, *16*, 125–148. [CrossRef]
18. Underwood, B.S.; Baek, C.; Kim, Y.R. Simplified viscoelastic continuum damage model as platform for asphalt t concrete fatigue analysis. *Transp. Res. Rec.* **2012**, *2296*, 36–45. [CrossRef]
19. Lee, H.J.; Kim, Y.R. Viscoelastic constitutive model for asphalt concrete under cyclic loading. *J. Eng. Mech.* **1998**, *124*, 32–40. [CrossRef]
20. Wang, R.; Yue, M.; Xiong, Y.; Yue, J. Experimental study on mechanism, aging, rheology and fatigue performance of carbon nanomaterial/SBS-modified asphalt binders. *Constr. Build. Mater.* **2021**, *268*, 121189. [CrossRef]
21. Wang, C.; Wang, H.; Zhao, L.; Cao, D. Experimental study on rheological characteristics and performance of high modulus asphalt binder with different modifiers. *Constr. Build. Mater.* **2017**, *155*, 26–36. [CrossRef]

22. AASHTO. Standard method of test for estimating fatigue resistance of asphalt binders using the linear Amplitude Sweep. In *AASHTO TP 101*; AASHTO: Washington, DC, USA, 2016.
23. Underwood, B.S. A continuum damage model for asphalt cement and asphalt mastic fatigue. *Int. J. Fatigue* **2016**, *82*, 387–401. [CrossRef]
24. Sabouri, M.; Mirzaiyan, D.; Moniri, A. Effectiveness of Linear Amplitude Sweep (LAS) Asphalt Binder Test in Predicting Asphalt Mixtures Fatigue Performance. *Constr. Build. Mater.* **2018**, *171*, 281–290. [CrossRef]
25. Ameri, M.; Seif, M.R.; Abbasi, M.; Khiavi, A.K. Viscoelastic fatigue resistance of asphalt binders modified with crumb rubber and styrene butadiene polymer. *Pet. Sci. Technol.* **2017**, *35*, 30–36. [CrossRef]